CFD Modeling of Crossflow Membrane Filtration – Integration of Filtration Model and Fluid Transport Model

E.H. Khor*, P. Kumar, Y. Samyudia

Department of Chemical Engineering, Curtin University of Technology, 98000 Miri, Sarawak, Malaysia
E-mail address: khor.ee.huey@stud.curtin.edu.my

Cross-flow membrane filtration has become a promising technique for waste-water treatment as compared to conventional treatment methods. One of the reasons is that the membrane techniques offer separation that can be achieved at ambient temperature with minimum energy. It is also an innovation for the application of cross-flow filtration in oil and gas industry especially as an integral part for the oil-in-water analysis of produced water prior to offshore disposal. However, good fouling control is essential for the efficiency of the cross-flow filtration unit. With the fact that membrane is not a passive entity, the understanding of particle deposition phenomena is vital for reducing fouling.

In this paper, filtration will be modeled through the relationship between hydrodynamics of the cross-flows and the transfer of flows across the membrane. The results of FLUENT simulated model are in good agreement with experimental results. Simulation results of the model are presented and then validated using experimental data for distilled (DI) water. From the model, some connecting variables are identified and established in this modeling work. By attaining these connections, optimization of membrane filtration can be achieved by adjusting the operating parameters.

Keywords: CFD modeling, Cross-flow membrane filtration, Produced water

I. INTRODUCTION

The determination of oil in produced water has been carried out for nearly two decades using solvent based extraction followed by infra-red quantification. However, following Freon being banned from used due to ozone depletion and the concerns over health and safety of its replacement Tetrachloroethylene (TTCE), OSLO-PARIS commission (OSPAR) implemented a new standard method across North Sea in 2007. The method is called OSPAR GC-FID method but it has its own limitation [1]. Our research is to incorporate the membrane filtration as part of oil-in water analysis so that dispersed and dissolved oil can be separated and thus allowing the oil and gas operators to comply with the stringent regulations. By doing this, we need to understand fouling or gel layer built up on the membrane so that our separation of both the oils can be complete. As such, we use FLUENT model to simulate the flow pattern inside the membrane to see the velocity and pressure distribution in the membrane cassette. Using this study, we are able to design an optimum condition for our oil separation.

Most of the works done on modeling are on the flow across the membrane and flux decline during filtration. Fouling models are based mainly on pore-blocking law, concentration polarization [9] and cake formation [6]. Particle deposition on the membrane had also been studied very extensively, such as in the modeling work of Elimelech and Song [10]. Several authors are also investigating the hydrodynamics of fluid relating to the membrane filtration process. Many of them model using the combination of Navier-Stokes equations and Darcy's law. Different approaches have been performed to simulate the combined models such as finite element method [7], finite difference scheme [5], and finite volume method [8]. Finite volume method and SIMPLE algorithm are commonly used in problems dealing with fluid flow. For our simulation, we want to study the flow pattern which is inside a concealed membrane. Our membrane is a rectangular small slits, anti-gravity flow type. We therefore use commercial finite volume package FLUENT models to visualize the flow pattern inside the membrane at steady state.

Our research work starts with model searching. From the many models available we had chosen two sub-models in our first stage. The first sub-model describes the fluid transport of flow parallel to the membrane while the second one describes the filtration across the membrane. The idea is to simulate the hydrodynamic characteristics which influence the solute deposition on the membrane. For our first stage, we use the models to simulate distilled (DI) water flow through membrane and validate with our experimental data. For the second stage, we use a third model (film theory model) to simulate the deposition of dispersed oil on the membrane which forms the gel layer. In this paper, it illustrates the first part of the study where filtration through membrane is studied at standard condition, room temperature and by using DI water.

II. NUMERICAL MODEL FORMULATION

Recall again, our simulation scope of this model is defined to be within the region of the membrane cassette (Fig. 2.1). For the first part of our modeling work, we model the flow of fluid through the slit between two membrane sheets (Fig. 1). The models done by Damak and coworkers [5] are modified to fit the membrane system that we are using. The flow in-let is from the bottom and out through the top of the rectangular slit of two membranes. According to Belfort and colleague [3] turbulent flow started at Re 4000 for porous tubes instead of Re 2100 in non-porous tubes. The dimensions in the membrane cassette are complicated and therefore it is difficult for Re calculations. However, due to the high pressure exerted at the retentate outlet, the flow is being disturbed and eddies are assumed to be formed. Flow in the porous slits is therefore expected to be in turbulence.

A. Flow regime in the slit

According to continuity equation and Navier-Stokes equation,

$$\frac{\partial u}{\partial x} + \frac{\partial v}{\partial y} = 0$$

The u-component is

$$\rho(u\frac{\partial u}{\partial x} + v\frac{\partial u}{\partial y}) = \mu(\frac{\partial^2 u}{\partial x^2} + \frac{\partial^2 u}{\partial y^2}) - \frac{\partial P}{\partial x} + \rho g_x$$

The v-component is

$$\rho(u\frac{\partial v}{\partial x} + v\frac{\partial v}{\partial y}) = \mu(\frac{\partial^2 v}{\partial x^2} + \frac{\partial^2 v}{\partial y^2}) - \frac{\partial P}{\partial y} + \rho g_y$$
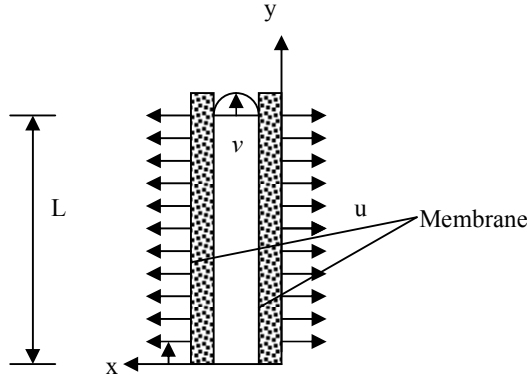
Figure 1: Slit between two sheets of membrane
(diagram is not proportional to the actual setup)

B. Flow regime at the porous wall

The momentum equation across porous zone, i.e. Darcy's law, is written as:

$$u = -\frac{\kappa}{\mu}\frac{\partial P}{\partial x}$$

Porous wall in the membrane is assumed to be homogenous and isotropic and the flow through porous wall can be treated as the boundary condition of the free flow through the tube.

1) Boundary Conditions

a) At the inlet, the inlet pressure is

$$p_0 = p_s + \frac{1}{2}\rho|\vec{v}|^2$$

Where p_o is the total pressure gauge at the inlet, p_s is the static pressure and v is the initial velocity which is 0.

b) At the exit, fully developed profile is assumed.

$$y = L, 0 < x < X: \quad \frac{\partial v}{\partial y} = 0; u = 0$$

c) At the axis of symmetry there are no momentum fluxes crossing the boundary.

$$x = 0, 0 \le y \le L: \quad \frac{\partial v}{\partial x} = 0, u = 0$$

d) At the porous wall, the wall suction velocity is given by Darcy's law and no slip velocity is applied, as follows,

$$x = X, 0 \le y \le L: \quad u = \frac{\kappa}{\mu}\frac{P - P_e}{e}, v = 0$$

$$u = R(P - P_e), \quad R = \frac{\kappa}{\mu}\cdot\frac{1}{e}$$

where κ is the permeability of the membrane, μ is the viscosity of the fluid and e is the thickness of the porous wall. These three parameters can be determined empirically and we conclude them in a term R, resistance. P_e is the external pressure (including osmotic pressure).

The numerical model assumed that the filtration is at steady state, with a turbulent flow type. There are six classical turbulence models in FLUENT i.e. mixing length, standard k-ε, RNG k-ε, realizable k-ε, Reynolds's stress and algebraic stress models [12].

For our case, standard k-ε model [13] was chosen as our membrane geometry is not complex and the flow is assumed to be fully turbulent and the effects of molecular viscosity are negligible. The standard k-ε model is a semi-empirical model based on model transport equations for the turbulence kinetic energy (k) and its dissipation rate (ε). The model transport equation for k is derived from the exact equation,

while the model transport equation for ε was obtained using physical reasoning and bears little resemblance to its mathematically exact counterpart. The transport equations for k and ε are as follows:

As
$$\mu_t = \rho C_\mu \frac{k^2}{\varepsilon};$$

$$\frac{\partial(\rho k)}{\partial t} + \frac{\partial}{\partial x_i}(\rho k u_i) =$$
$$\frac{\partial}{\partial x_j}\left[\left(\mu + \frac{\mu_t}{\sigma_k}\right)\frac{\partial k}{\partial x_j}\right] - \rho \overline{u_i u_j}\frac{\partial u_j}{\partial x_i} - \rho\varepsilon$$

And

$$\frac{\partial(\rho\varepsilon)}{\partial t} + \frac{\partial}{\partial x_i}(\rho\varepsilon u_i) =$$
$$\frac{\partial}{\partial x_j}\left[\left(\mu + \frac{\mu_t}{\sigma_\varepsilon}\right)\frac{\partial\varepsilon}{\partial x_j}\right] + C_{1\varepsilon}\frac{\varepsilon}{k}(-\rho\overline{u_i u_j}\frac{\partial u_j}{\partial x_i}) - C_{2\varepsilon}\rho\frac{\varepsilon^2}{k}$$

$C_{1\varepsilon}$ and $C_{2\varepsilon}$ are constants. σ_k and σ_ε are the turbulent Prandtl numbers for k and ε, respectively. When differential pressure (DP) is increased from 0.5bar to 2bar, with an interval of 0.5; the turbulent intensity decreases as described in Tab. 2.

As mentioned in previous section, we use the Darcy's equation in modeling the filtration of distilled water across the membrane. In FLUENT, Darcy's equation is under the porous jump boundary condition with the numeric model described as follows:

$$\Delta p = -\left(\frac{\mu}{\alpha}v\right)\Delta m$$

P is the Trans-membrane Pressure (TMP), μ is the viscosity of the fluid, α is the permeability of the medium, v is the filtration flux, m is the thickness of the membrane.

In our FLUENT geometry, we used a representation of 2 slices of membrane separating 3 rectangular compartments to model the flow pattern inside the membrane cassette as illustrated in Fig. 1.

III. EXPERIMENTAL SET-UP

For experimental validation, Sartocon Slice Cassette containing Polyethersulfone (PESU) membrane with 50kD molecular-weight-cut-off (MWCO) is used. The dimensions of the cassettes are given in the diagram (Fig 2.1). Each membrane cassette contains 20 slices of membrane sheets. The distance between each membrane sheets is approximately 1mm (Fig 2.2).
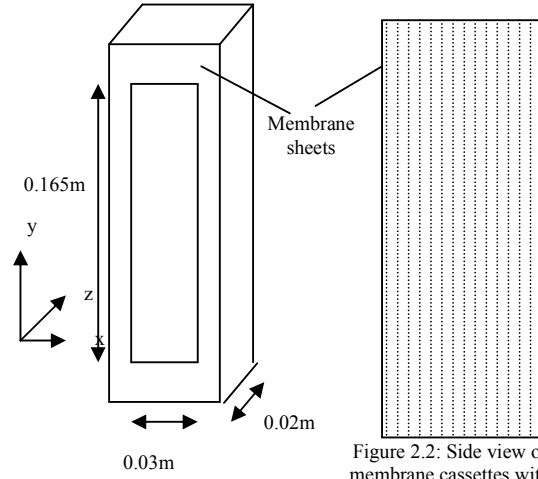

Figure 2.1: A dimension of membrane cassette

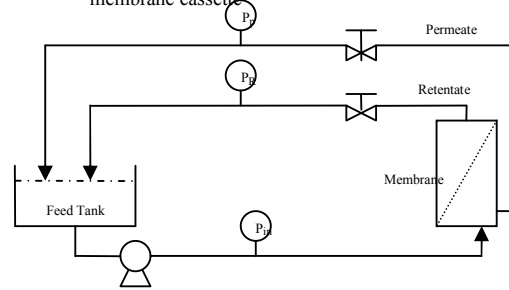Figure 2.2: Side view of membrane cassettes with illustration of membrane sheets

Figure 3: Experimental set-up for cross-flow membrane filtration

The empirical data of the permeability of the membrane, κ is calculated based on the formula,

$$\kappa = u/(P.\mu)$$

Where u is the permeate flux, P is the trans-membrane pressure (TMP) and μ is the viscosity of the fluid in this case $0.001 \text{kgm}^{-1}\text{s}^{-1}$.

Trans-Membrane Pressure,
$$TMP = [(P_{feed} + P_{ret})/2] - P_{per}$$
Differential Pressure,
$$DP = P_{feed} - P_{ret}$$

P_{feed}, P_{ret}, and P_{per}, are Feed pressure, Retentate pressure and Permeate pressure respectively. Thickness of membrane, e is 0.1mm based on the information given by the manufacturer. All these information are included in the simulation. Experiments are performed at TMP = 2.75 bar and Re between 4000 and 10000 by varying the operating pressures using the experimental set-up shown in Fig. 3. Permeate and feed velocities are measured at DP 0.5, 1.0, 1.5, and 2.0. The simulated results from FLUENT are then validated with experimental data.

IV. RESULTS AND DISCUSSIONS

Darcy's equation and Navier-Stokes transport equations associated with the boundary conditions given in Section II were solved by using finite volume method from a commercial software FLUENT.

DP	TMP	Feed mass flowrate	Permeate mass flowrate	Retentate mass flowrate
0.5	2.75	0.04952	0.04584	0.00368
1.0	2.75	0.06910	0.04450	0.02510
1.5	2.75	0.08504	0.04233	0.04271
2.0	2.75	0.09375	0.04100	0.05280

Tab.1 shows the experimental data for mass flowrate for DP 0.5 to 2.0 at constant TMP

Tab. 1 shows how the experimental feed, permeate and retentate mass-flowrate (kg/s) changes under different operating differential pressure and Trans-membrane Pressure (TMP). The conditions (turbulence intensity) are adjustable to fit the experimental data.
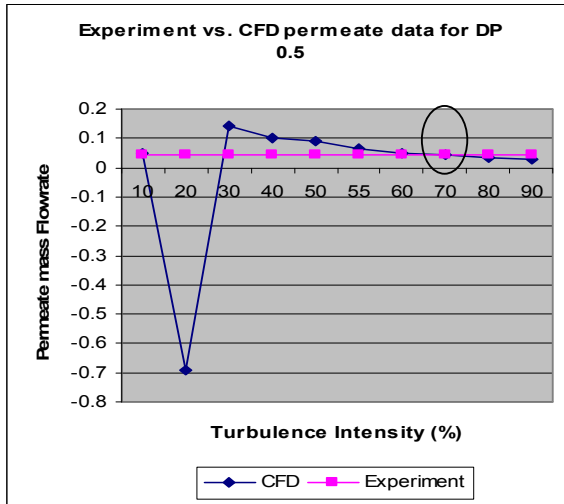

Fig 4: CFD vs. Experimental data at different turbulence intensity for DP 0.5
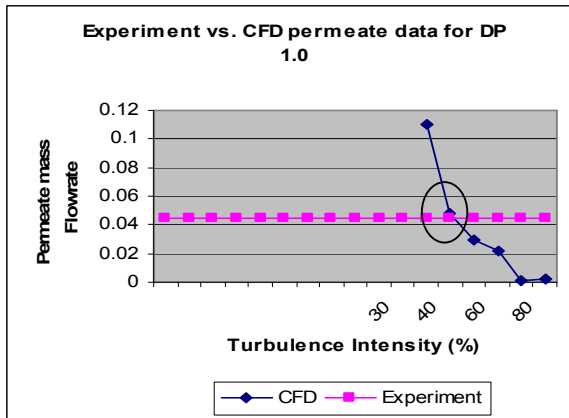

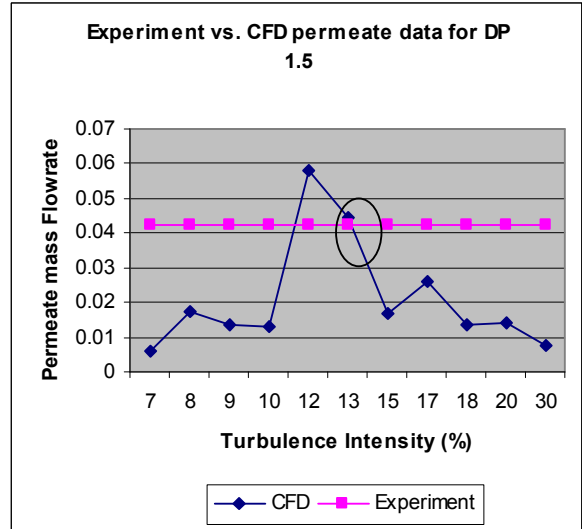Fig 5: CFD vs. Experimental data at different turbulence intensity for DP

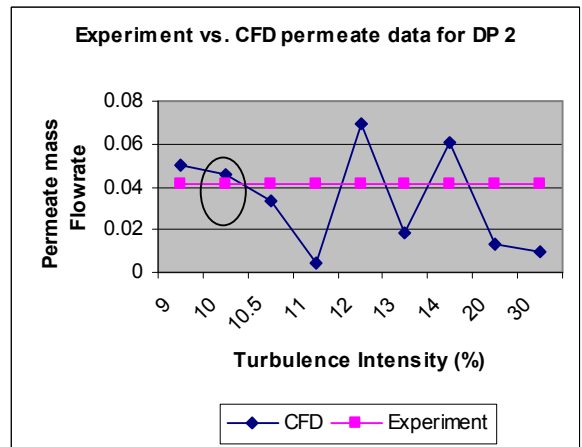Fig 6: CFD vs. Experimental data at different turbulence intensity for DP 1.5

Fig 7: CFD vs. Experimental data at different turbulence intensity for DP 2.0

Fig. 4 to 7 shows the effect of the changes in turbulence intensity towards the permeate fluxes. However the most suitable turbulence intensity conditions to have the CFD data verified with experimental data are identified and listed in Tab. 2.

Tab. 2 shows the CFD and experimental results for feed, retentate and permeate mass flowrates. To avoid confusions, Fig. 8 was plotted for permeate only for both CFD data and experimental data. From the CFD results all the DPs fits well with the experimental results and they are within the range of 10% in difference.

		CFD			Experiment		
DP	Condition	Feed	Permeate	Retentate	Feed	Permeate	Retentate
0.5	70	0.04950	0.04214	0.00736	0.04952	0.04584	0.00368
1.0	40	0.06910	0.04812	0.02113	0.06910	0.04450	0.02510
1.5	13	0.08504	0.04457	0.04048	0.08504	0.04233	0.04271
2.0	10	0.09375	0.04557	0.06009	0.09375	0.04100	0.05280

*Condition – turbulence intensity (%)

Table 2: Experimental data and CFD data for mass-flowrates (kg/s) of feed, retentate and permeate for various DPs
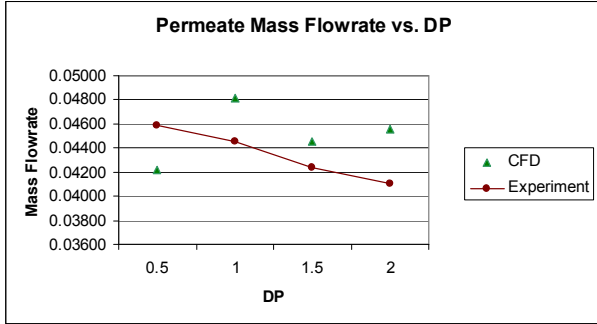

Figure 8: Comparison of permeate flux from experiment and CFD

Fig. 9 shows the velocity plot at the outlet for DP 0.5 at TMP 2.75. The velocity plot from -0.5 to 0.5mm are the retentate fluxes and the rest are permeate fluxes. This diagram shows that permeate fluxes are higher than the retentate fluxes. As DP increases from 0.5 to 2 (Fig 9 to 12), we can see that the trend is reversed, as retentate fluxes increases whereas the permeate fluxes decreases. This trend is the same as the trend from our experimental data. As DP increases, fluid flow in the retentate slit becomes faster and thus less permeation through the membrane. The CFD result at DP 1.0 is much lower than the experimental data which may be attributed to the turbulent flow assumption. Nevertheless, the simulation is good enough as it predicts the same trend as the experimental data.

From Tab. 2, it can be seen that as DP increases, the turbulence intensity decreases. This indicates that lower DP has higher turbulence intensity than higher DP. The calculation of turbulence intensity is by the equation, [12]

$$I = 0.16(\text{Re})^{-\frac{1}{8}}$$

Therefore from the equation, we will be able to calculate and find out the Re for the flow in the retentate slit.
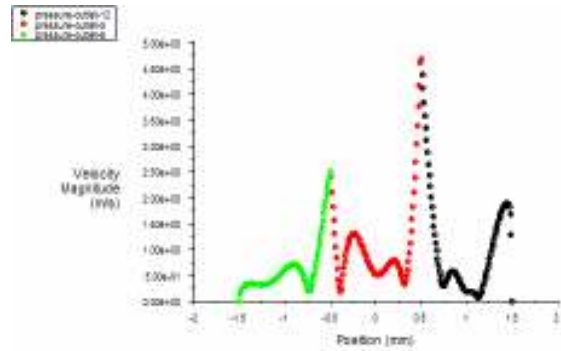

Figure 9: Velocity plot at the outlet for condition DP=0.5, TMP=2.75 at 70% turbulence intensity.
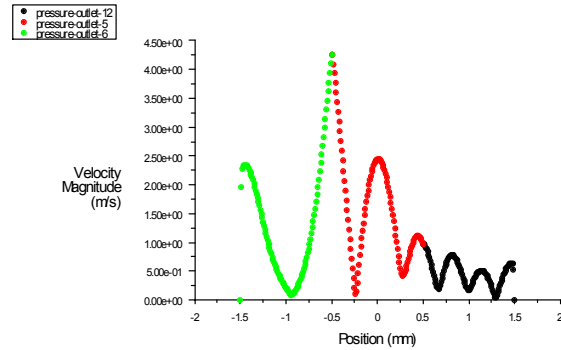

Figure 10: Velocity plot at the outlet for condition DP=1.0, TMP=2.75 at 40% turbulence intensity.
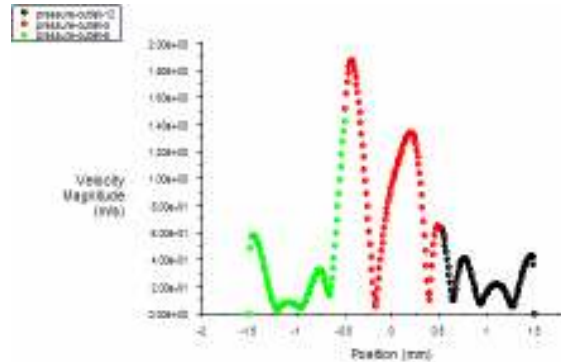

Figure 11: Velocity plot at the outlet for condition DP=1.5, TMP=2.75 at 13% turbulence intensity.
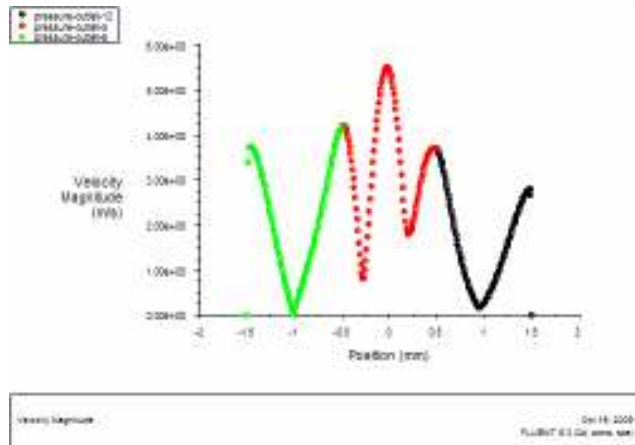
Figure 12: Velocity plot at the outlet for condition DP=2.0, TMP=2.75 at 10% turbulence intensity.

V. CONCLUSIONS

In conclusions, the CFD can predict the permeate flux with a reasonable accuracy for the deionized water filtration. From the simulation it can be seen that the differential pressure and velocity is interconnected. Lower DP contributes to higher turbulence intensities. Therefore to obtain a higher permeate flux we need to operate at lower DP and vice versa.

VI. REFERENCES

[1] E.H. Khor, Y. Samyudia, "The Study of Mass Transfer Coefficient in Membrane Separation For Produced Water", International Journal Chemical Engineering, 2009, in press

[2] R.W. Baker, "Membrane Technology and Applications", McGraw-Hill, 2004.

[3] G. Belfort., N. Nagata "Fluid mechanics and crossflow filtration: some thoughts", Desalination, vol. 53, 1985, pp. 57-79.

[4] P.L.T. Brian "Mass Transport in Reverse Osmosis. Desalination by Reverse Osmosis. U. Merten, ed. ed., MIT Press, Cambridge, MA, 1966.

[5] K. Damak, A. Ayadi, B. Zeghmati, P. Schmitz "A new Navier-Stokes and Darcy's law combined model for fluid flow in crossflow filtration tubular membranes. Desalination, vol. 161, 2004, pp. 67-77.

[6] L. Huang, M.T. Morrissey "Fouling of membranes during microfiltration of surimi wash water: Roles of pore blocking and surface cake formation", Journal of Membrane Science, vol. 144, 1998, pp.113-123.

[7] V. Nassehi, "Modelling of combined Navier-Stokes and Darcy flows in crossflow membrane filtration", Chem. Eng. Sci., 53, 1998, pp. 1253-1265.

[8] A. Pak, T. Mohammadi, S.M. Hosseinalipour, V. Allahdini "CFD modeling of porous membranes", Desalination, vol. 222, 2008, pp. 482-488.

[9] M.C. Porter, "Concentration Polarization with Membrane Ultrafiltration", Ind. Eng. Chem. Prod. Res. Develop., vol. 11, 1972, pp. 234 - 248.

[10] L. Song, M. Elimelech "Particle deposition onto a permeable surface in laminar flow", Journal of Colloid and Interface Science, vol. 173, 1995, pp. 165-180.

[11] G. Van den Berg, C.A. Smolder, "The boundary-layer resistance model for unstirred ultrafiltration. A new approach", Journal of Membrane Science, vol. 40, 1989, pp. 149-172.

[12] FLUENT 6.3 User-guide, Sept 2006

[13] B.E. Launder, D.B. Spalding "Lectures in Mathematical Models of Turbulence", Academic Press, London, England, 1972.